Efficient Trapping of HNO by Deoxymyoglobin

Filip Sulc, Chad E. Immoos,[†] Dmitry Pervitsky, and Patrick J. Farmer*

Contribution from the Department of Chemistry, University of California, Irvine, California 92697-3900

Received July 29, 2003; E-mail: pfarmer@uci.edu

Abstract: Nitrosyl hydride, HNO, also commonly termed nitroxyl, is a transient species that has been implicated in the biological activity of nitric oxide, NO. Herein, we report the first generation of a stable HNO−metal complex by direct trapping of free HNO. Deoxymyoglobin (Mb−Fe(II)) rapidly reacts with HNO produced from the decomposition of methylsulfonylhydroxylamine (MSHA) or Angeli's salt (AS) in aqueous solutions from pH 7 to pH 10, forming an adduct, Mb−HNO. The unique ^{1}H NMR signal of the Fe-bound HNO at 14.8 ppm allows definitive proof of its formation. The generation of Mb−HNO and quantification of various myoglobin byproducts were accomplished by correlation of ^{1}H NMR, UV−vis, and EPR spectroscopies. Typically, the maximum Mb−HNO yield obtained is 60−80%; competitive side reactions with byproducts as well as the further reactivity of the Mb−HNO decrease the overall yield. At pH 10, the observed rate of Mb−HNO generation by trapping HNO from MSHA is close to that for MSHA decomposition; kinetic simulations give a lower limit to the bimolecular rate of trapping as 1.4×10^4 M^{-1} s^{-1}. The binding of HNO to deoxymyoglobin is rapid and essentially irreversible, which suggests that the biological activity of nitroxyl may be mediated by its reactivity with ferrous heme proteins such as myoglobin and hemoglobin.

Nitrosyl hydride (HNO), also commonly termed nitroxyl, is a transient species that has been implicated in the biological activity of nitric oxide, NO.[1,2] HNO also has extensive physiological activity of its own, for instance, as an inhibitor of aldehyde dehydrogenase, and a possible protective agent for heart disease.[3,4] It is short-lived in aqueous solution due to near diffusion-controlled dimerization between pH 2 and pH 11, eq 1.[5] Recent work has led to a reevaluation of the oxidation potential and pK_a of HNO,[6,7] and there remains much debate about its biological relevance.[8]

$$2HNO \rightarrow N_2O + H_2O \qquad (1)$$

A variety of metalloproteins have been suggested to play roles in the biological and physiological activity of HNO. Transient nitroxyl intermediates have long been proposed in the catalytic cycles of the heme-based nitrite and nitric oxide reductases.[9,10] An Fe-bound nitroxyl intermediate has been spectroscopically identified during turnover of P450nor, a fungal nitric oxide reductase.[11] Free nitroxyl is a byproduct of P450$_{nos}$ turnover in the absence of biopterin,[12] and has been suggested as a substrate of Cu, Zn superoxide dismutase.[13−16] The reaction of free HNO with ferric forms of the oxygen binders hemoglobin and myoglobin directly yields the ferrous nitrosyl adducts,[17] but its reactions with the physiological ferrous states of these proteins is complicated and has remained controversial.[18,19] Recently, it has been suggested that the reactivity of NO and

† Present address: Department of Chemistry, Duke University, Durham, NC 27710.

(1) Hughes, M. N. *Biochim. Biophys. Acta* **1999**, *1411*, 263.

(2) Stamler. J. S.; Singel, D. J. Loscalzo, J. *Science* **1992**, *258*, 1898.

(3) (a) DeMaster, E. G.; Redfern, B.; Nagasawa, H. T. *Biochem. Pharm.* **1998**, *55*, 2007−2015. (b) Demaster, E. G.; Redfern, B.; Quast, B. J.; Dahlseid, T.; Nagasawa H. T. *Alcohol* **1997**, *14*, 181−189.

(4) (a) Paolocci, N.; Saavedra, W. F.; Mirannda, K. M.; Martignani, C.; Isoda, T.; Hare, J. M.; Espey, M. G.; Fukuto, J. M.; Feelisch, M.; Wink, D. A. Kass, D. A. *Proc. Natl. Acad. Sci. U.S.A.* **2001**, *98*, 10463−10468. (b) Pagliaro, P.; Mancardi, D.; Rastaldo, R.; Penna, C.; Gattullo, D.; Miranda, K. M.; Feelisch, M.; Wink, D. A.; Kass, D. A.; Paolocci, N. *Free Radical Biol. Med.* **2003**, *34*, 33−43.

(5) (a) Bazylinski, D. A.; Hollocher, T. C. *Inorg. Chem.* **1985**, *24*, 4285−4288. (b) Hughes, M. N.; Cammack, R. *Methods Enzymol.* **1999**, *301*, 279−287.

(6) (a) Bartberger, M. D.; Liu, W.; Ford, E.; Miranda, K. M.; Switzer, C.; Fukuto, J. M.; Farmer, P. J.; Wink, D. A.; Houk K. N. *Proc. Natl. Acad. Sci. U.S.A.* **2002**, *99*, 10958−10963. (b) Bartberger, M. D.; Fukuto, J. M.; Houk, K. N. *Proc. Natl. Acad. Sci. U.S.A.* **2001**, *98*, 2194−2198.

(7) (a) Shafirovich, V.; Lymar, S. V. *Proc. Natl. Acad. Sci. U.S.A.* **2002**, *99*, 7342−7345. (b) Shafirovich, V.; Lymar, S. V. *J. Am. Chem. Soc.* **2003**, *125*, 6547−6552.

(8) (a) Miranda, K. M.; Espey, M, G.; Yamada, K.; Krishna, M.; Ludwick, N.; Kim, S.; Jourd'heuil, D.; Grisham, M. B.; Feelisch, M.; Fukuto, J. M.; Wink, D. A. *J. Biol. Chem.* **2001**, *276*, 1720−1727. (b) Naughton, P.; Hoque, M.; Green, C. J.; Foresti, R.; Motterlini, R. *Cell. Mol.* **2002**, *48*, 885−894.

(9) Einsle, O.; Messerschmidt, A.; Huber, R.; Kroneck, P. M. H.; Neese, F. *J. Am. Chem. Soc.* **2002**, *124*, 11737−11745.

(10) (a) Averill, B. A. *Chem. Rev.* **1996**, *96*, 2951. (b) Ye, R. W.; Averill, B. A.; Tiedje, J. M. *Appl. Environ. Microbiol.* **1994**, *60*, 1053. (c) Averill, B. A.; Tiedje, J. M. *FEBS Lett.* **1982**, *138*, 8.

(11) (a) Shiro, Y.; Fujii, M.; Iizuka, T.; Adachi, S. I.; Tsukamoto, K.; Nakahara, K.; Shoun, H. *J. Biol. Chem.* **1995**, *270*, 1617. (b) Daiber, A.; Nauser, T.; Takaya, N.; Kudo, T.; Weber, P.; Hultschig, C.; Shoun, H.; Ullrich, V. *J. Inorg. Biochem.* **2002**, *88*, 343−352.

(12) Rusche, K. M.; Spiering, M. M.; Marletta, M. A. *Biochemistry* **1998**, *37*, 15503−15512.

(13) Hobbs, A. J.; Fukuto, J. M.; Ignarro, L. J. *Proc. Natl. Acad. Sci. U.S.A.* **1994**, *91*, 10992−10996.

(14) (a) Murphy, M. E.; Sies, H. *Proc. Natl. Acad. Sci. U.S.A.* **1991**, *88*, 10860−10864. (b) Klotz, L. O.; Sies, H. *Methods Enzymol.* **2002**, *349*, 101−106.

(15) (a) Liochev, S. I.; Fridovich, I. *Arch. Biochem. Biophys.* **2002**, *402*, 166−171. (b) Liochev, S. I.; Fridovich, I. *J. Biol. Chem.* **2001**, *276*, 35253−35257. (c) Liochev, S. I.; Fridovich, I. *Free Radical Biol. Med.* **2003**, *34*, 1399−1404.

(16) (a) Nelli, S.; McIntosh, L.; Martin, W. *Eur. J. Pharm.* **2001**, *412*, 281−289. (b) Nelli, S.; Hillen, M.; Buyukafsar, K.; Martin, W. *Br. J. Pharm.* **2000**, *131*, 356−362.

(17) Bazylinski, D. A.; Hollocher, T. C. *J. Am. Chem. Soc.* **1985**, *107*, 7982−7986.

HNO with heme proteins is "orthogonal", i.e., that NO mainly interacts with ferrous hemes and HNO with ferric hemes.[20]

Isolable metal complexes of HNO are rare, and are typically air and water sensitive.[21-28] A notable exception is the HNO adduct of ferrous myoglobin,[28] Mb–HNO or {Mb–HNO},[8] using the Enemark/Feldman notation,[29] which has a half-life of months in anaerobic, aqueous solution. The ^{1}H NMR spectrum of Mb–HNO exhibits a sharp proton signal at 14.8 ppm, confirmed by splitting of the peak in the H^{15}NO adduct. Using this unique diamagnetic signal, we have recently determined the solution structure of the Mb–HNO heme pocket by NOE and COSY NMR methods.[30]

To date, all reported HNO–transition-metal complexes have been obtained by insertion or redox reactions of NO-related species. For example, the initial route to Mb–HNO was by Cr(II) reduction of the nitrosyl adduct Mb–NO or {Mb–NO}[7] using the Enemark/Feldman notation, as in eq 2.[28] Herein, we report the first example of a stable HNO complex formed by direct trapping of free HNO by ferrous myoglobin, deoxymyoglobin or Mb–Fe(II), in aqueous solutions as in eq 3. As free HNO is short-lived in solution, it was generated in these experiments by decomposition of methylsulfonylhydroxylamine (MSHA), CH_3SO_2NHOH, in alkaline-buffered solutions, or by decomposition of Angeli's salt (AS), $Na_2N_2O_3$, in neutral solutions.

$$Mb-NO + Cr(II) + H^+ \rightarrow Mb-HNO + Cr(III) \quad (2)$$

$$Mb-Fe(II) + HNO \rightarrow Mb-HNO \quad (3)$$
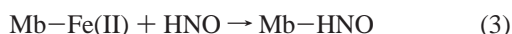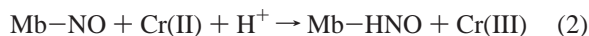
Experimental Section

All solvents were of ACS chemical grade (Fisher) and were used without further purification unless otherwise indicated. Horse skeletal muscle myoglobin (95–100%) was obtained from Sigma and purified on Amicon with Millipore YM-30 and YM-10 ultrafiltration membranes. Angeli's salt was obtained from Cayman Chemical Co. and used without further purification. MSHA was prepared according to Brinks, and recrystallized several times;[31] Anal. Calcd (Found) for CH_5NO_3S: C, 10.81 (11.01); H, 4.54 (4.59). Water was purified to a specific resistance of 18 mΩ^{-1} in a Barnstead Nanopure water purification system. All experiments were performed at room temperature, 23 ± −2 °C, in 50 mM phosphate buffer for pH 7–8 or 50 mM carbonate buffer for pH 10; all experiments were performed at room temperature, 23 ± 2 °C. All other chemicals were purchased from Sigma or Fisher, and used as obtained.

^{1}H NMR spectra were collected on a Bruker Avance 500 MHz spectrometer. Chemical shifts are referenced to 2,2′-dimethyl-2-silapentane-5-sulfonate (DSS) via the solvent signal. Solvent suppression was achieved by direct saturation during the relaxation delay. The Mb–HNO peak integrations were typically monitored every 64 scans (ca. 6 min). A Hewlett-Packard 8453 UV–vis spectrophotometer was used for optical measurements. EPR spectra were recorded on a Bruker EMX 300 spectrophotometer equipped with an Air Products LTR3 liquid helium cryostat. Experimental conditions were as follows: microwave frequency, 9.475 GHz; microwave power, 0.5 mW; modulation amplitude, 4.57 G; modulation frequency, 100 kHz; field sweep rate, 11.92 G/s; time constant, 0.0256 ms; receiver gain, 1.0 × 10^4.

Generation of Deoxymyoglobin. Typically, a 40-fold excess of sodium dithionite was added to a metmyoglobin, Mb–Fe(III), solution under anaerobic conditions and the resulting deoxymyoglobin purified on a Sephadex G-25 size exclusion chromatography column equilibrated at experimental pH. For ^{1}H NMR experiments, the resulting deoxymyoglobin was concentrated to approximately 5 mM, with addition of D_2O to 10%.

Reaction of Deoxymyglobin with MSHA. MSHA was added in 1, 1.5, 2, and 3 molar ratios to a solution of ca. 5–6 mM deoxymyoglobin, and aliquots were withdrawn to allow time-course UV–vis absorbance and ^{1}H NMR spectral measurements. In some cases, G-25 column filtration was used to inhibit further reactions of the Mb–HNO product. Quantification of Mb–NO concentrations in specific aliquots were obtained by comparison of doubly integrated EPR spectra of the products with that of an authentic Mb–NO sample formed by reaction of Mb–Fe(III) with excess dithionite/nitrite.

Reaction of Deoxymyoglobin with Angeli's Salt. Deoxymyoglobin was reacted with various stoichiometries of AS, as above, and time-based UV–vis and ^{1}H NMR spectra were collected. Reactions were run under concentrated, 4 mM at pH 7, and dilute, 40 μM at pH 8, conditions. Aliquots were removed from the reaction mixture, purified by G-25 column filtration, and then concentrated for ^{1}H NMR analysis. Aliquots of the purified samples were examined by UV–vis. Separate kinetic experiments at lower concentrations were performed for UV–vis analysis.

Kinetic Analysis. The rates of MSHA decomposition and Mb–HNO formation under identical conditions were obtained by fitting time-based ^{1}H NMR integrations with the following considerations. First, the percentage of Mb–NO contaminant was determined by EPR in aliquots with maximum Mb–HNO, and then the integral values of the nitrosyl hydride peak due to Mb–HNO formation were lowered by this value (i.e., the whole curve was multiplied by the fractional percent of Mb–HNO). For MSHA disappearance, the integrals of the methyl groups of MSHA and $MeSO_2^-$ were followed, and the average sum of their integrations was set to unity, i.e., equal to the total MSHA derivative concentration. The fractional concentrations of both Mb–HNO and MSHA were then multiplied by their initial concentrations, 5.7 mM, to obtain concentration vs time plots. An initial estimate of the rate of decomposition of MSHA was determined by a natural log of concentration vs time plot, and this value was used as a starting point in the subsequent simulations using REACT for Windows, Version 1.2, as described in the text.[32]

(18) Bazylinski, D. A.; Goretski, J.; Hollocher, T. C. *J. Am. Chem. Soc.* **1985**, *107*, 7986–7989.
(19) (a) Doyle, M. P.; Mahapatro, S. N.; Broene, R. D.; Guy, J. K. *J. Am. Chem. Soc.* **1988**, *110*, 593–599. (b) Doyle, M. P.; Mahapatro, S. N. *J. Am. Chem. Soc.* **1984** *106*, 3678–9.
(20) Miranda, K. M.; Nims, R. W.; Thomas, D. D.; Espey, M. G.; Citrin, D.; Bartberger, M. D.; Paolocci, N.; Fukuto, J. M.; Feelisch, M.; Wink, D. A. *J. Inorg. Biochem.* **2003**, *93*, 52–60. (b) Miranda, K. M.; Paolocci, N.; Katori, T.; Thomas, D. D.; Ford, E.; Bartberger, M. D.; Espey, M. G.; Kass, D. A.; Feelisch, M.; Fukuto, J. M.; Wink, D. A. *Proc. Natl. Acad. Sci. U.S.A.* **2003**, *100*, 9196–9201.
(21) Roper, W. R.; Grundy, K. R.; Reed, C. A. *Chem. Commun.* **1970**, 1501–1503.
(22) Wilson, R. D.; Ibers, J. A. *Inorg. Chem.* **1979**, *18*, 336–343.
(23) Southern, J. S.; Hillhouse, G. L.; Rheingold, A. L. *J. Am. Chem. Soc.* **1997**, *119*, 12406–12407.
(24) Southern, J. S.; Green, M. T.; Hillhouse G. L.; Guzei, I. A.; Rheingold, A. L. *Inorg. Chem.* **2001**, *40*, 6039–6046.
(25) Melenkivitz, R.; Hillhouse, G. L. *Chem. Comm.* **2002**, 660–661.
(26) Sellmann, D.; Gottschalk-Gaudig, T.; Haussinger, D.; Heinemann, F. W.; Hess, B. A. *Chem.—Eur. J.* **2001**, *7*, 2099–2103.
(27) Melenkivitz, R.; Southern, J. S.; Hillhouse, G. L.; Concolino, T. E.; Liable-Sands, L. M.; Rheingold, A. L. *J. Am. Chem. Soc.* **2002**, *124*, 12068–12069.
(28) Lin, R.; Farmer, P. J. *J. Am. Chem. Soc.* **2000**, *122*, 2393–2394.
(29) The Enemark and Feltham nomenclature for NO and HNO complexes denotes the combined number of electrons in the metal d-orbitals and N–O π* orbitals, as described in Enemark, J. H.; Feltham, R. D. *Coord. Chem. Rev.* **1974**, *13*, 339–406.
(30) Sulc, F.; Ma, D.; Fleisher, E.; Farmer, P. J.; La Mar, G. N. *J. Biol. Inorg. Chem.* **2003**, *8*, 348–352.
(31) Brink, K.; Gombler, W.; Bliefert, C. *Z. Anorg. Allg. Chem.* **1977**, *429*, 255–260.
(32) *REACT for Windows, Version 1.2*; Manka, M. J., Ed.; Alchemy Software, Wesley: Chapel, FL, 2001; as described in Braun, W.; Herron, J. T.; Kahaner, D. K. *Int. J. Chem. Kinet.* **1988**, *20*, 51–62.

Results and Discussion

HNO and Its Transition-Metal Adducts. Despite the high interest in biological activity of nitric oxide, the fundamental chemistry of its one-electron-reduced form, nitroxyl or HNO, remains poorly understood. For instance, very recent experimental and theoretical work suggests that the pK_a of HNO is >11.4,[6,7] decidedly higher than the previously accepted value of 4.7.[33] Therefore, it is predicted to exist almost exclusively in its protonated form under physiological conditions.

Similar confusion over pK_a is evident in previous descriptions of the bonding of HNO to transition-metal complexes. Much theoretical effort was given to explain an apparent pK_a of ca. 7 for the HNO ligand in a family of complexes of the form $(HNO)ReCl(CO)_2(PR_3)_2$, which was thought to break the rule that metal coordination lowers the pK_a of protic ligands.[24]

Many reduced nitrosyl complexes of iron porphyrin complexes have been generated and characterized electrochemically in organic solvents,[34,35] but such species are not long-lived in aqueous solution.[36] For example, the one-electron-reduced product of $(NO)Fe(tpps)^{4-}$ in aqueous pH 6 solution had a measured half-life of ca. 2 s.[37] The first experimental evidence for a stable HNO adduct of Mb came from electrochemical experiments which showed a highly reversible, one-electron reduction of Mb−NO at high pH.[38] Subsequently, chemical or electrochemical reductions of Mb−NO yielded stable solutions of Mb−HNO, with a unique peak at 14.8 ppm in ^{1}H NMR spectra, consistent with protonation at the nitrogen.[28] By measurement of the ^{1}H NMR signal, Mb−HNO samples have a half-life in anaerobic solutions of more than six months; in these stable solutions, the intensity of the HNO peak is unchanged from pH 6 to pH 10 relative to peaks assigned to nonionizable protons, such as those of the methyl groups of Val 68 at −0.9 and −2.7 ppm. A possible source of the stability is direct hydrogen bonding between the bound HNO and the distal pocket histidine, His 64, as is suggested in the solution Mb−HNO structure determined by NMR.[30] With the stability and structure of Mb−HNO established, its formation from direct reaction of Mb−Fe(II) with free HNO was investigated using two commonly used nitroxyl precursors, as described below.

Reactions with MSHA. MSHA is an analogue of the well-studied Piloty's acid, and it produces HNO through first-order decomposition at high pH, as in eqs 4 and 5.[39]

$$CH_3SO_2NHOH + OH^- \rightleftharpoons CH_3SO_2NHO^- + H_2O \quad (4)$$

$$CH_3SO_2NHO^- \rightleftharpoons CH_3SO_2^- + HNO \quad (5)$$

The reaction of MSHA with deoxymyoglobin in a 1:1 molar ratio at pH 10 yields Mb−HNO as the major product, as demonstrated by ^{1}H NMR, Figure 1. As stated above, both free nitroxyl and its myoglobin adduct are expected to be protonated
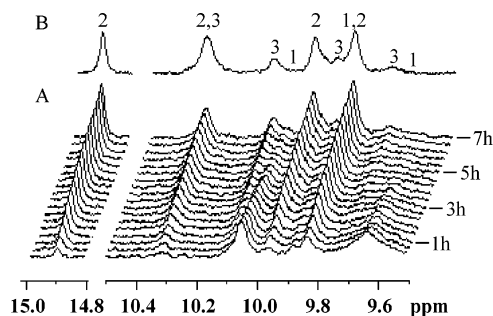
(33) Gratzel, V. M.; Taniguchi, S.; Henglein, A. *Ber. Bunsen-Ges. Phys. Chem.* **1970**, *74*, 1003.
(34) (a) Lancon, D.; Kadish, K. M. *J. Am. Chem. Soc.* **1982**, *104*, 2042. (b) Lancon, D.; Kadish, K. M. *J. Am. Chem. Soc.* **1983**, *105*, 5610.
(35) Liu, Y. M.; Desilva, C.; Ryan, M. D. *Inorg. Chim. Acta* **1997**, *258*, 247.
(36) Barley, M. H.; Takeuchi, K.; Meyer, T. J. *J. Am. Chem. Soc.* **1986**, *108*, 5876.
(37) tpps = *meso*-tetrakis(*p*-sulfonatophenyl)porphyrinate. Seki, H.; Hoshino, M.; Kounose, S. *J. Chem. Soc., Faraday Trans.* **1996**, *92*, 2579.
(38) Bayachou, M.; Lin, R.; Cho, W.; Farmer, P. J. *J. Am. Chem. Soc.* **1998**, *120*, 9888−9893.
(39) King, S. B.; Nagasawa, T. *Methods Enzymol.* **1999**, *301*, 211−220.

Figure 1. ^{1}H NMR spectra of the reaction of deoxymyoglobin and stoichiometric MSHA at pH 10 with peaks of various myoglobin adducts in the 9.4−10.4 ppm region labeled as (1) deoxymyoglobin, (2) Mb−HNO, and (3) Mb−NO. Spectra A show the growth of the nitroxyl peak at 14.8 ppm and changes in the meso proton region every 24 min over 7 h. Spectrum B shows the same reaction mixture after 43 h.
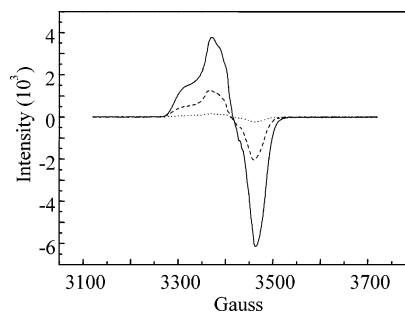

Figure 2. Electron paramagnetic resonance (EPR) spectra of Mb−Fe(II) (dotted line), a Mb−HNO sample contaminated with Mb−NO (dashed line) from stoichiometric reaction of MSHA with Mb−Fe(II), and an authentic sample of Mb−NO (solid line). Spectra are normalized to total Mb concentration in each sample from protein absorbance at 280 nm.

at pH 10. The time course of the ^{1}H NMR spectra illustrates the loss of paramagnetic Mb−Fe(II), and concurrent formation of signals indicative of Mb−HNO and Mb−NO from 9.5 to 10.5 ppm. Decreases in peaks assignable to methyl groups of MSHA and increases in peaks assigned to its decomposition product, $MeSO_2^-$, are a measure of the generation of HNO (Supporting Information, Figure S1).

Quantification of paramagnetic species is problematic by NMR; therefore, a combination of methods was applied to the generated reaction mixtures. UV−vis analysis was used to measure the loss of Mb−Fe(II), and EPR spectra of the product following column purification allowed estimation of Mb−NO content, Figure 2. In the 1.5:1 reaction, Figure 3, combined ^{1}H NMR, UV−vis, and EPR analysis gave estimated concentrations at the specific time points marked: (A) after 20 min the estimated concentrations were 90% Mb−Fe(II) and 10% Mb−HNO; (B) after 180 min the estimated concentrations were 35% Mb−Fe(II), 50% Mb−HNO, and 15% Mb−NO; (C) after 340 min the estimated concentrations were 70% Mb−HNO and 30% Mb−NO. The presence of significant amounts of Mb−NO after 180 min indicates that both the NO and HNO adducts are formed concurrently in these experiments. Significant efforts were made to reduce the Mb−NO contaminant without success.[40] The coproduction of NO during HNO generation from Piloty's acid

(40) Efforts included repeated recrystallization of the MSHA to high purity by ^{1}H NMR and the addition of excess EDTA to inhibit possible metal-catalyzed NO oxidation; no effective decrease in Mb−NO contaminant was observed in either case.
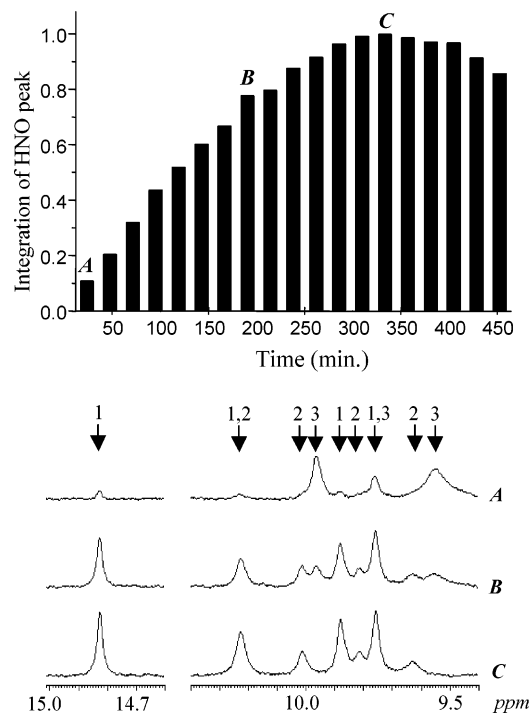
Figure 3. Top: Integration of the Mb—HNO peak at 14.8 ppm over the course of 1:1.5 reaction of deoxymyoglobin with MSHA at 5.7 mM and pH 10, as in Figure 1. Integration is relative to a maximum value, which corresponds to ca. 70% conversion to Mb—HNO. Bottom: NMR spectra of samples at specific time points in illustrating peaks due to Mb—HNO (1), Mb—NO (2), and Mb—Fe(II) (3).
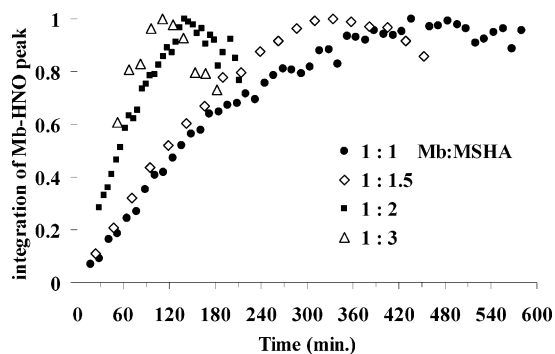

Figure 4. Integration of the Mb—HNO peak at 14.8 ppm over the course of different stoichiometries of MSHA to Mb—Fe(II) (5–6 mM) and pH 10, as in Figure 3. Integration is relative to a maximum value, which ranges from 60% to 80% conversion.

has been previously noted,[41] and may be due to HNO oxidation or disproportionation.[42]

Reactions carried out with concentrations of MSHA varying from stoichiometric to 3-fold excess all obtain similar maximum Mb—HNO yields, typically from 60% to 80%, with Mb—NO being the main contaminant. At higher MSHA concentrations, the maxima are obtained at shorter times; afterward the Mb—HNO concentration decreases rapidly, Figure 4. Without purification by column chromatography, the Mb—HNO yield also decreases over time and the concentration of Mb—NO increases. The apparent further reactivity of Mb—HNO with free HNO and/or NO, as well as with other small-molecule decomposition products, diminishes the overall yield.

(41) Zamora, R.; Grzesiok A.; Weber H.; Feelisch M. *Biochem. J.* **1995**, *312*, 333–339.
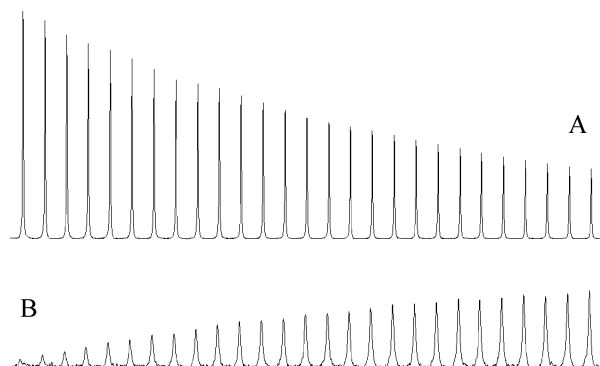(42) Mahapatro, S. Personal communication.

Figure 5. Changes observed in ¹H NMR signals over 5¹/₂ h, illustrating (A) the decomposition of MSHA, as measured by the methyl substituent at ca. 2.9 ppm, and (B) the growth of Mb-HNO, as illustrated by the signal of the HNO proton at 14.8 ppm, under identical conditions at pH 10. Both experiments were started ca. 17 min into the reaction with sequential spectra taken in 12 min intervals.
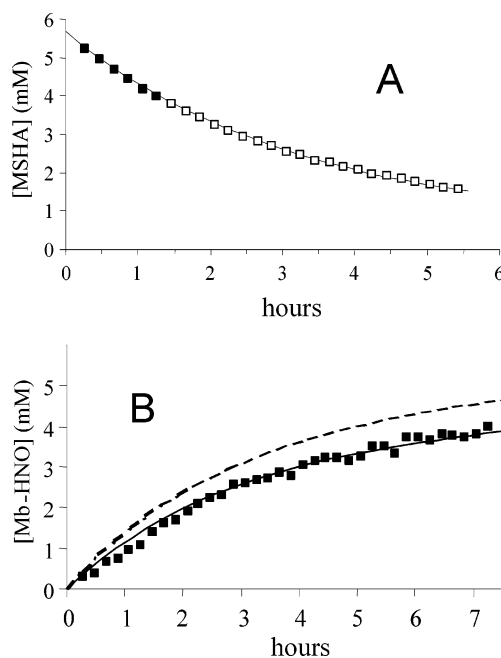

Figure 6. Determination of rates of MSHA decomposition and Mb—HNO formation. (A) [MSHA] vs time derived from disappearance of the methyl peak at 2.9 ppm. The rate constant k_5 ($\sim$8.0 $\times$ 10⁻⁵ M⁻¹ s⁻¹) was determined by fitting values obtained in the initial $\sim$5000 s of the reaction (solid line) and modeled with k_1 (fitted data not shown); all data points were used for determination of k_{-5} ($\sim$3.0 $\times$ 10³ M⁻¹ s⁻¹) to obtain the modeled line shown. (B) [Mb—HNO] vs time derived on the basis of normalized integration (solid squares) of the Mb—HNO peak at 14.8 ppm. The dashed line represents the total HNO produced by MSHA decomposition, and the solid line represents the modeled rate of Mb—HNO formation ($k_3 \approx$ 2.3 $\times$ 10⁴ M⁻¹ s⁻¹) as described in the text.

The rate of reaction of Mb—Fe(II) with HNO, eq 3, can be estimated from the observed formation of Mb—HNO relative to the decomposition of MSHA using the normalized integrals of the ¹H NMR signals in Figure 5. As the decomposition of MSHA is under equilibrium with its products, a series of natural log([MSHA]/[MSHA]ₒ) vs time plots were derived using iteratively larger data sets. Within the first 5000 s, the determined rates remain relatively constant at ca. 7.7 $\times$ 10⁻⁵ M⁻¹ s⁻¹ (Supporting Information, Figure S2A); including eq 1 as a side reaction ($k_1 = 1.8 \times 10^9$ M⁻¹ s⁻¹) in kinetic simulations yielded $k_5 = 8.0 \times 10^{-5}$ s⁻¹ (Supporting Information, Figure S2B). Iterative fitting of the complete data set (20000 s) gave
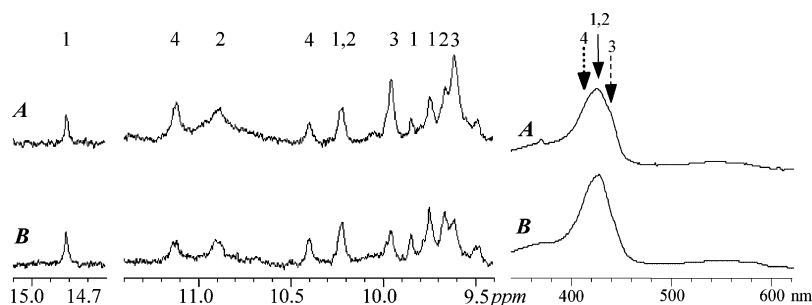
Figure 7. (Left) NMR spectra of stoichiometric reaction of AS with Mb−Fe(II) at 4 mM concentration, pH 7, illustrating peaks due to Mb−HNO (labeled 1), Mb−NO (labeled 2), Mb−Fe(II) (labeled 3), and Mb−Fe(III) (labeled 4). Spectrum A was taken after 4 min, spectrum B after 6 min. (Right) UV−vis spectra in the Soret region of both samples, with labeling as above: Mb−Fe(III) (411 nm), Mb−HNO (423 nm), Mb−NO (421 nm), Mb−Fe(II) (434 nm).

the rate of the back reaction, k_{-5}, as 2.0×10^3 M^{-1} s^{-1}, Figure 6A. Using these rates, the data for Mb−HNO formation in Figure 5B were fit to give a bimolecular rate, $k_3 = 1.4 \times 10^4$ M^{-1} s^{-1}, Figure 6B. We consider this rate a low estimate due to the concurrent formation of Mb−NO, and note that, at the end of the stoichiometric reactions (ca. 7 h), Mb−Fe(II) is not discernible by UV−vis or ^{1}H NMR.

Reactions with AS. Angeli's salt decomposes from pH 4.4 to pH 8.13 (as HN$_2$O$_3^-$) to give HNO and NO$_2^-$ with a half-life of 17 min ($k = 6.8 \times 10^{-4}$ s^{-1}), eq 6.[5]

$$HN_2O_3^- \leftrightharpoons HNO + NO_2^- \qquad (6)$$

Stoichiometric reaction of Angeli's salt with concentrated Mb−Fe(II) (4 mM) at pH 7 generated a complex mixture of products which included transient formation of Mb−Fe(III), Figure 7. Combined ^{1}H NMR, UV−vis, and EPR analysis give estimated concentrations at 4 min as 30% Mb−NO/Mb−HNO, 50% Mb−Fe(II), and 20% Mb−Fe(III). At 6 min, the estimated concentrations were 50% Mb−NO/Mb−HNO, 20% Mb−Fe(II), and 30% Mb−Fe(III); after half a day, the sample was >90% Mb−NO.

Several previous investigations of the reactivity of AS with heme proteins observed similar complicated reactivity, but in these reports the affinity of HNO for ferrous hemes was either discounted or largely underestimated.[17,18] Our work has shown that the binding of HNO to Mb−Fe(II) is effectively irreversible, as the preformed adduct is stable for months in solution from pH 6 to pH 10.[28,30] Therefore, we postulated that the complex product mixtures must result from competing reactivity of the nitrite byproduct, e.g., eq 7.

$$Mb−Fe(II) + NO_2^- + H^+ \rightarrow Mb−Fe(III) + NO + OH^- \qquad (7)$$
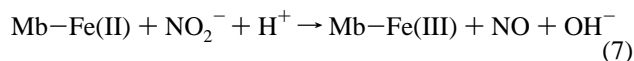
As previously noted for hemoglobin,[43] the rate of reaction of Mb−Fe(II) with nitrite is zero order in protein, but first order in nitrite and protons (Supporting Information, Figures S2 and S3).[44] Under the above reaction conditions (4 mM, pH 7), the rate of eq 7 is ca. 10^2-fold greater than that of eq 6, leading to significant buildup of Mb−Fe(III). Raising the pH to 8 decreases the rate of reaction with nitrite but does not affect the unimolecular decomposition of HN$_2$O$_3^-$, eq 6.[5] Likewise, dilution diminishes the overall rate of reaction to allow maximization of the Mb−HNO yield, obtained by isolation and

(43) (a) Doyle, M. P.; Pickering, R. A.; DeWeert, T. M.; Hoekstra, J. W.; Pater, D. *J. Biol. Chem.* **1981**, *256*, 12393. (b) Doyle, M. P.; Pickering, R. A.; Dykstra, R. L.; Cook, B. R. *J. Am. Chem. Soc.* **1982**, *104*, 3392−3397.
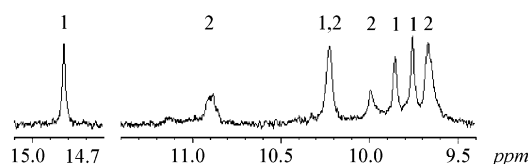(44) Immoos, C. E. Dissertation, University of California, Irvine, 2002.

Figure 8. NMR spectrum of purified and concentrated protein after reaction of AS with Mb−Fe(II), at a 1.5:1 stoichiometry, at 40 μM concentration, pH 8, for 30 min. Combined ^{1}H NMR, UV−vis, and EPR analysis gives estimated concentrations after 30 min, 70% Mb−HNO (labeled 1) and 30% Mb−NO (labeled 2).
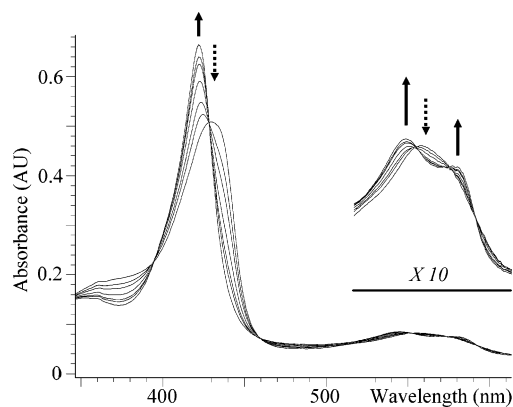

Figure 9. Absorbance spectra of the reaction of Mb−Fe(II) with a 1.5-fold excess of AS at 5 μM concentration, pH 8, over 25 min. Solid arrows indicate increasing absorbances due to Mb−HNO (Soret at 423 nm), and dotted arrows indicate loss of absorbance due to Mb−Fe(II) (Soret at 434 nm).

column purification. Indeed, at 40 μM protein concentrations and pH 8, a 1.5:1 reaction of AS with Mb−Fe(II) gave ca. 60% isolated Mb−HNO after 30 min, Figure 8. A time-course UV−vis absorbance, shown in Figure 9, demonstrates a relatively clean conversion to a Mb−HNO/Mb−NO mixture with no formation of Mb−Fe(III).

Survey of Reactivity. An initial survey of the reactivity of Mb−HNO has been performed as an attempt to delineate the subsequent reactions that limit the overall yield of HNO in trapping experiments. As previously reported, Mb−HNO is a powerful reductant and may be oxidized to Mb−NO by reaction with stoichiometric methyl viologen.[28] Prepurified anaerobic solutions of Mb−HNO, which are stable for months under N$_2$ atmosphere, will decompose upon exposure to air over a period of minutes to generate Mb−Fe(III). Most interesting are reactions with NO or NO$_2^-$ solutions. In excess both reagents cause a conversion to Mb−NO; the conversion occurs over minutes under a NO atmosphere,[45] while the reaction with nitrite is much slower and apparently pH dependent. Careful study of

these and other reactions of the HNO adduct are underway, and will be the subject of a subsequent paper.

Physiological Implications. Our results demonstrate that the binding of HNO to Mb−Fe(II) is rapid and irreversible. HNO is isoelectronic with dioxygen, and on the basis of the stability of purified Mb−HNO, the affinity of Mb−Fe(II) for HNO is much greater than that of its native substrate. This new method of synthesizing HNO−metal adducts may have physiological implications in the action of pro-nitroxyl drugs such as cyanamide and AS. In the latter case, we have demonstrated that the byproducts of the HNO precursor decomposition can have a considerable effect on the observed chemistry. Further complications arise from the subsequent reactivity of the ferrous HNO adduct. Clearly, any consideration of the physiological effect of HNO must take into account its binding by ferrous hemes and possible following reactions of the bound adduct.

(45) Lin, R. Dissertation, University of California, Irvine, 2001.

Supporting Information Available: Further descriptions of the NMR analysis of various Mb species, details of the kinetic analysis, a brief comparison of literature values for the rate of HNO dimerization, and a description of the mechanistic investigations on the reaction of deoxymyoglobin with nitrite. This material is available free of charge via the Internet at http://pubs.acs.org.

JA0376184